Nano-honeycomb electrode based QCM sensor and its application for PPI detection

Nano-honeycomb electrode based QCM sensor and its application for PPI detection

Naoto Asai, Naohiro Matsumoto, Nozomi Kazama, Yasuo Nagaoka, Takaaki Sumiyoshi,
Tomohiro Shimizu, Shoso Shingubara, Takeshi Ito[*]

Abstract—An anodic aluminon oxide (AAO)-based nano honeycomb electrode was fabricated on a quartz crystal to increase the surface area binding with analyte for use as a sensing device in a quartz crystal microbalance (QCM) to monitor the protein-protein interactions (PPIs). As examples, we detected PPIs of anti-Bcl-2 and Bcl-2, and Bcl-2 and Bax in real time. A sensor with a flat Au electrode showed a tiny frequency shift upon sample injection. However, our fabricated device could detect Bcl-2 and Bax in sequence. Frequency shifts corresponding to the binding of Bcl-2 to anti Bcl-2, and that of Bax to Bcl-2 increased linearly.

Index Terms—Biosensor, quartz crystal microbalance (QCM), protein-protein interaction, real time detecting.

I. INTRODUCTION

Protein-protein interactions (PPIs) play key roles in a variety of biological processes such as intercellular and intracellular signal transduction [1, 2]. Although dysregulated PPIs are potent targets in drug discovery, there is a limited number of potential PPI inhibitors [3, 4]. For example, many monoclonal antibodies (mAbs) are therapeutic drugs that act via the inhibition of intercellular PPIs. However, mAbs are not appropriate for disrupting intracellular PPIs because of their poor cell permeability, therefore the application of these drugs is limited [5, 6]. To overcome this hurdle, the discovery of low-molecular-weight compounds that inhibit intracellular PPIs has attracted the interest of medicinal chemists [4, 7].

To evaluate PPIs, the binding and dissociation of compounds to the target protein and the combined multiplier are measured using conventional techniques such as enzyme-linked immunosorbent assay (ELISA) [8-10]. ELISA can be used to analyze a large number of samples; however, it requires professional skills and takes a long time because of the need for labeling and incubation. In addition, ELISA is not suitable for real-time monitoring. On the other hand, surface plasmon resonance (SPR) [11-13] and quartz crystal microbalance (QCM) methods [14-16] are concise, cost-effective, and

N. Asai, N. Matsumoto, N. Kazama, Y. Nagaoka, T. Sumiyoshi, T. Shimizu, S. Shingubara and T. Ito are with Graduate School of Science and Engineering, Kansai University, Suita, Osaka, 564-8680 Japan. (e-mail: t.ito@kansai-u.ac.jp)

powerful methodologies for monitoring real-time PPIs. Since these techniques are performed using flow injection methods, pharmaceutical researchers use them for high-throughput screening. Since SPR systems involve complicated optical systems such as a goniometer, they are generally quite large. In contrast, a QCM is simple, convenient, cost-effective, and small owing to the use of common electronic device technologies coupled with a microfluidic device. A QCM includes an AT-cut quartz crystal, whose fundamental resonant frequency is mainly determined by the thickness of the quartz crystal. When the target material is attached on the electrode surface of the quartz crystal, the resonant frequency decreases and the magnitude of the frequency shift is proportional to the change in mass. Therefore, the development of a high-sensitivity electrode for PPIs is necessary for the effective screening of intracellular PPI inhibitors. Here we describe a high-sensitivity electrode with a nano-honeycomb structure and its application detection of PPIs between anti B-cell lymphoma (Bcl)-2 and Bcl-2 and between Bcl-2 and Bcl-2-associated X protein (Bax).

In our program to develop novel methodology to detect PPI inhibitors, we have focused on the interaction between Bcl-2 and Bax. Inhibiting this interaction will lead to the apoptosis of cancer cells. Members of the Bcl-2 family of proteins are essential in regulating apoptosis [17]. The effects of Bcl-2, Bcl-extra large (xL), and Bax (molecular weight: 36.74 kDa) on the regulation of the apoptosis of mesangial cells have been investigated by many groups [18-20]. When Bax directly binds to the pocket of Bcl-2 (molecular weight: 36.63 kDa), apoptosis is suppressed. Therefore, Bcl-2 inhibitors are potent candidates for the treatment of cancer. Most research groups have used ELISA and western blot analysis to detect Bcl-2-related interactions [21-23] and a few groups have attempted to use SPR [24]. However, no group has ever shown the possibility of using a QCM to measure the interaction of Bcl-2 and Bax.

To improve the sensitivity of a QCM, three approaches have been followed: (1) using very thin quartz crystal, (2) using nanoparticles to increase the weight and (3) increasing the surface area to enable the attachment of a larger quantity of the target materials. Using the first strategy, the fundamental frequency was increased to 150 MHz by fabricating extremely thin quartz (thickness: 25 µm) without an electrode or wiring to apply an AC voltage [25]. In this case, the quartz was too thin for it to be used in practical applications. In addition, the proposed QCM-based sensor required a special AC source. On
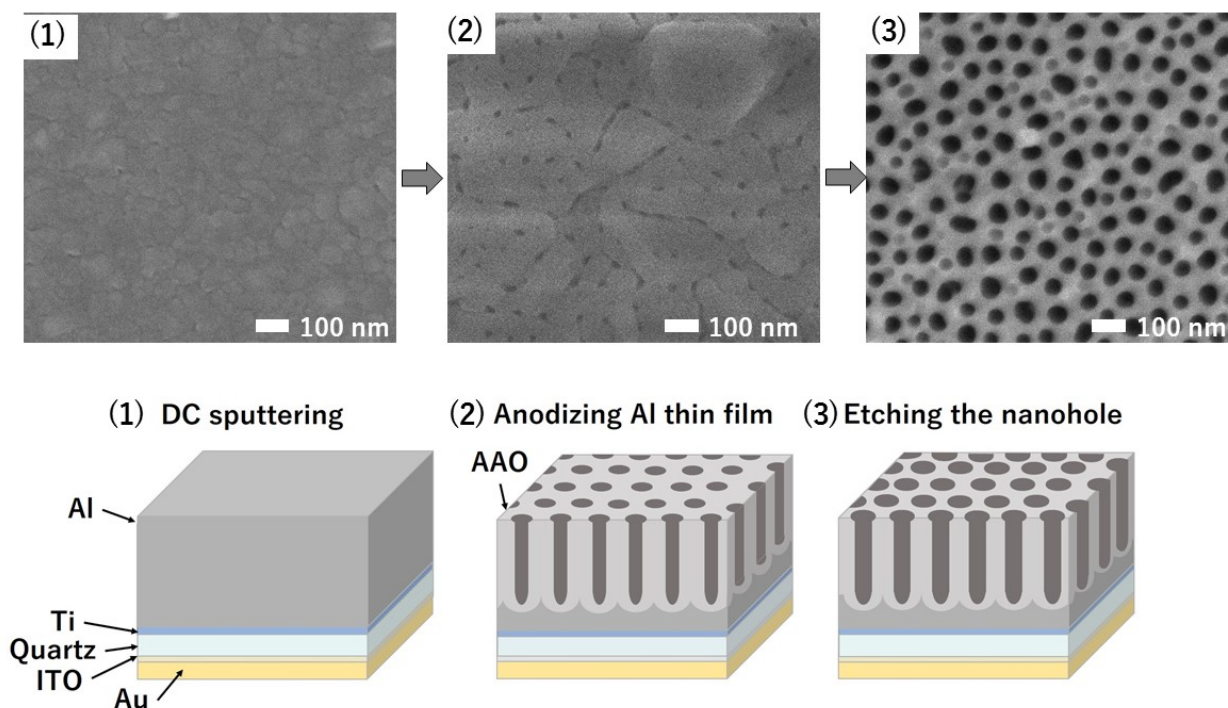
Fig.1 Upper: SEM images corresponding to process steps (1)-(3). Lower: Schematic figure of process used to fabricate nano-honeycomb electrode on quartz crystal.

the second strategy, gold nanoparticles and magnetic nanoparticles were used [26, 27]. These techniques need extra preparation procedure for functionalization of nanoparticles. Using the third strategy, nanostructures were introduced to increase the surface area for binding with analyte [28-30]. In this case, sensor preparation is easy and conventional. We have focused on this strategy, which was realized using a three-dimensional (3D) nanostructure based on anodic aluminum oxide (AAO). The AAO nanostructure is obtained by anodizing only aluminum under a suitable potential in an electrolyte solution with a counter electrode [31]. Then, a self-organized nanohole array having a triangular lattice is formed in the downward direction with the nanoholes having a high aspect ratio which we refer to as a nano-honeycomb structure. The aspect ratio is controllable via the anodic conditions, such as the electrolyte solution, applied voltage, anodization time, and solution temperature [32]. Appropriate conditions result in a nanostructure with a self-assembled nanohole array and high aspect ratio using a conventional fabrication process. Therefore, an AAO nano-honeycomb structure having a large area can be fabricated at a low cost.

II. EXPERIMENTAL

A. Fabricating nano-honeycomb electrode on the quartz crystal

A schematic diagram of the fabrication process for a quartz crystal substrate coated with a nano-honeycomb electrode is shown in Fig. 1. An aluminum thin film of 700 nm thickness and a titanium thin film of 25 nm thickness were sputtered on a quartz substrate (fundamental frequency: 9 MHz) using DC

magnetron sputtering equipment. The Ti film was used as an adhesion layer. The diameter of the electrode was set to 5 mm. All the reagents used to fabricate the AAO nanostructure and form the self-assembled monolayer (SAM) were purchased from Wako Pure Chemical Industries. The AAO nanostructure was obtained by anodization of the Al thin film in 0.3 M oxalic acid. A potential of 40 V was applied between the Al thin film and a glassy carbon counter electrode. These anodic conditions are suitable for the formation of a self-assembled nanohole array [33]. After the anodization, the nanohole diameter was increased to 70 nm by dipped in 5 wt% phosphoric acid. The nanostructure was fabricated on one side of the quartz substrate. The other side was coated with indium tin oxide (ITO) of 25 nm thickness and Au of 100 nm thickness by sputtering. Stop-view
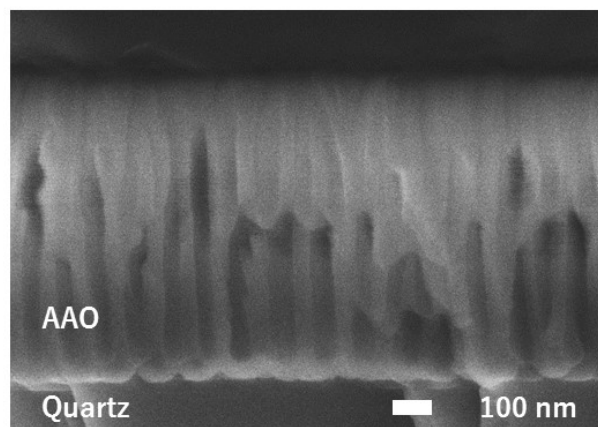

Fig.2 Cross-section SEM image of fabricated AAO-based nano-honeycomb layer on the quartz substrate.

scanning electron microscopy (SEM) images taken during the process are shown in Fig. 1. After the anodization (2), small holes with a diameter of 30 nm were distributed irregularly on the top surface of the Al. Although the two-step anodization of Al would have produced a regular array of nanoholes, the thickness of the Al layer was insufficient for it to be performed. After the etching of the nanoholes, their diameter was increased to about 70 nm. Fig. 2 shows a cross-section SEM image taken after the etching (3). The AAO nanostructure was vertically well aligned and uniformly distributed on the substrate. The thickness of the AAO nanostructure was about 700 nm according to the SEM image. These growth conditions of the AAO structure were previously optimized and reported elsewhere [34]. The diameter and growth direction at the top of the AAO nanostructure were less uniform than those at the bottom because the initially formed small nanoholes were electrolyzed and grew vertically downward along the roughness of the as-sputtered Al thin film [35].

B. Biomolecules immobilization

To use the fabricated device for biosensing, some biomaterials were coated on the device such as antigens. An antigen can bind an antibody specifically. However, a biomolecule cannot directly attach to an AAO surface since AAO does not have a functional group that can immobilize biomolecules. Thus, we used a SAM with terminated amino group. The QCM sensor coated with a nano-honeycomb electrode was immersed in toluene including 3-aminopropyltriethoxysilane (toluene: 3-aminopropyltriethoxysilane = 99:1) for 1 h at 65 °C. After sonicating with 2-propanol, it was baked for 30 min at 110 °C to induce the dehydration condensation of a SAM. Then, a stable SAM was formed on the surface of the AAO-nanostructure. Anti-Bcl-2 (mAbs), Bcl-2, and bovine serum albumin (BSA) were purchased from Funakoshi Co., Ltd. 4-(2-hydroxyethyl)-1-piperazineethanesulfonic acid (HEPES, 10 mM, pH=7.6) was used as a buffer solution. 25 μL of anti-Bcl-2 (100 μg/mL) was added dropwise to the electrode for 30 min to bind it on the AAO-nanostructure. After washing with HEPES buffer to prevent the nonspecific adsorption of anti-Bcl-2, 25 μL of BSA solution (0.01 wt%) was added dropwise over 30 min to avoid nonspecific adsorption. Then, it was rinsed by the HEPES buffer again. Here, the anti-Bcl-2 and BSA were immobilized by amide linkages between the amino group on the SAM layer and the carboxyl group included in the biomolecules [36].

On the contrast, QCM sensor with Au flat electrode was used as a benchmark. The electrode was coated by only dropping solution including anti-Bcl-2 (100 μg/mL) and BSA (0.01 wt%) in order. These proteins bound on the Au electrode through thiol binding.

C. PPI detection using flow injection analysis

These QCM sensors were set on a measurement cell, which was connected to a flow injection system. The measurement cell had a flow cell, an inlet, and an outlet made of poly(dimethylsiloxane) (PDMS). The depth and diameter of the flow cell were 1 and 5.5 mm, respectively. The QCM-based sensor with the measurement cell was connected to a QCM analyzer (QCM 922A, Seiko EG&G) then placed in a constant-temperature chamber to maintain the room temperature. The overtone number was set to three (n=3); thus, the operating frequency was 27 MHz. The frequency shift was monitored with a flow rate of 5 μl/min, which was controlled by a syringe pump. We measured the frequency shift corresponding to the antigen-antibody reaction by injecting Bcl-2 firstly and different concentrations of Bax in sequence, which demonstrated to monitor the interaction between Bcl-2 and Bax. All the injection volume was set as 50 μl.

III. RESULTS AND DISCUSSION

The resonance characteristics of the fabricated QCM chip during the preparation process are shown in Fig. 3. Here, Fig. 3(a) shows the characteristics for the QCM sensor coated with the nano-honeycomb electrode and Fig. 3(b) shows those for the QCM sensor with a flat Au electrode. All the measurements were carried out in air. In the case of the nano-honeycomb electrode, the resonance frequency decreased during the process, and the frequency shift after binding of the antibody was about 1200 Hz. In the case of
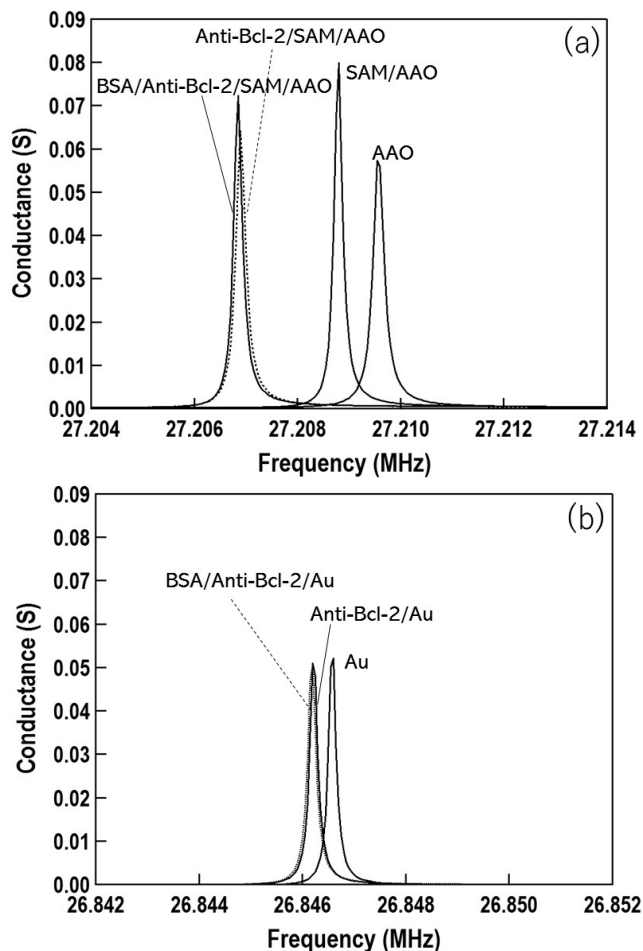

Fig.3 Resonance characteristics of the AAO-based nano-honeycomb electrode (a) and flat Au electrode (b) during the preparation process.

the flat Au electrode, the resonant frequency decreased by about 400 Hz after antibody binding. In fact, the frequency shift on the nano-honeycomb electrode was three times larger than that on the flat surface in the antibody-binding process. The result indicated that the mass load of the antibody increased owing to the large surface area of the nano-honeycomb structure. In addition, the resonant frequency did not change after the binding of BSA for both electrodes. The data indicate that there was very little space for the binding of BSA to the electrode surface. These results show that the mass load increased during the process because the biomolecules were accurately immobilized on the surface of the nano-honeycomb structure.

The interaction between an antigen (Bcl-2) and an antibody (anti-Bcl-2) and interaction between two proteins of Bcl-2 and Bax were evaluated using the QCM. In fact, we first carried out real-time monitoring of the frequency shift corresponding to the adhesion of Bcl-2 to anti-Bcl-2 followed that for the adhesion of Bax to Bcl-2. To evaluate the effect of the large surface area due to the nanostructure, a commercially available QCM sensor with a gold electrode on both sides of the quartz crystal was used as a reference. It had a fundamental frequency of 9 MHz but a working frequency was set as 27 MHz. In this case, a flat Au electrode had a diameter of 5 mm. These conditions were exactly the same as those for the fabricated QCM device with AAO nanostructure. In this experiment, we injected Bcl-2 (10 µg/mL) after the resonance frequency reached the steady state. After measuring the interaction between anti-Bcl-2 and Bcl-2, Bax (10 µg/mL) was also injected to monitor the interaction between Bcl-2 and Bax. The obtained time-dependent frequency shift is shown in Fig. 4. Arrows in figure show the time on the sample injections. The resonance frequency on both electrodes started to decrease approximately 20 min after the Bcl-2 injection. In the case of the flat Au electrode, after reaching minimum, the resonance frequency increased to almost the
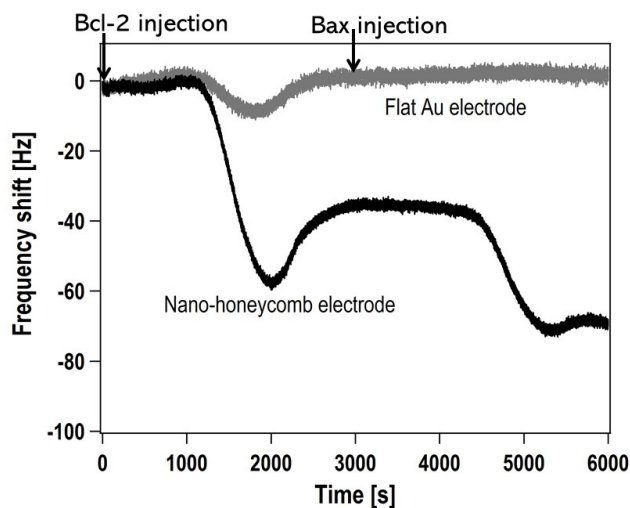

Fig.4 Time-dependent frequency shift corresponding to Bcl-2 and Bax injection. Gray and black lines represent the flat Au electrode and the nano-honeycomb electrode, respectively.
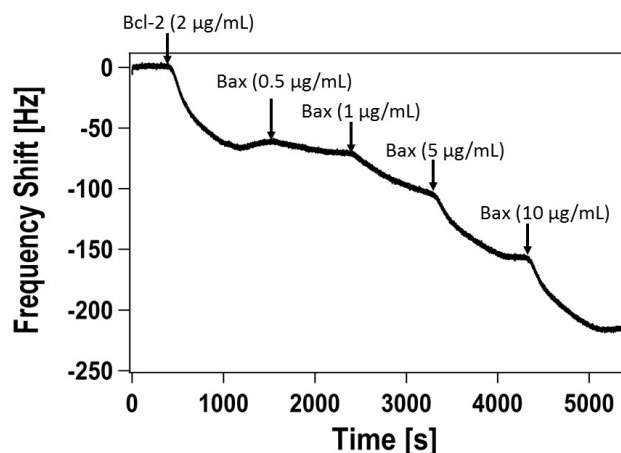

Fig.5 Time-dependent frequency shift after the injection of Bcl-2 (2 µg/mL), subsequently injection of different concentrations of Bax (0.5, 1.0, 5.0, 10 µg/mL) in sequence.

same as that before the injection. Then, there was hardly any frequency shift after Bax injection since Bcl-2 was not adsorbed on the anti-Bcl-2. In contrast, after reaching a minimum, the resonance frequency increased but remained below the initial value for the nano-honeycomb electrode, indicating that the QCM sensor coated with the nano-honeycomb electrode was able to detect the interaction of Bcl-2 and anti-Bcl-2. In this case, the frequency shift was about 36 Hz. In addition, the resonant frequency also started to decrease about 23 min after Bax injection. The frequency shift was about 37 Hz.

Then we measured the frequency shifts dependent with the concentration both on anti Bcl-2 and Bcl-2 interaction, and Bcl-2 and Bax interaction. As an example, Fig. 5 shows the time-dependent frequency shift after the injection of Bcl-2 (2 µg/mL), subsequently injection of different concentrations of Bax (from 0.5 to 10 µg/mL) in sequence. Here, arrows in the figure show the injection samples. As the results, we could affirm the frequency shift on the Bax concentration of 0.5 µg/mL. In addition, absolute frequency shift increased with the Bax concentration. Frequency shifts on the antigen-antibody interaction on Fig. 5 was larger than that on Fig. 4, even though the concentration of Bcl-2 on Fig .5 was lower than that on Fig. 5. The results indicate that the sensor has variable sensitivity. Primitive analytical curves of anti Bcl-2 and Bcl-2 interaction, and Bcl-2 and Bax were shown in supporting information as Fig. S1 and Fig. S2, respectively. Here, the plots were average of twice experiments. Frequency shifts on the binding of Bcl-2 to anti Bcl-2 increased linearly in the range from 0.5 to 10 µg/mL. In similar, frequency shifts on the binding of Bax to Bax increased linearly in the range from 0.5 to 10 µg/mL. A gradient of the analytical curve on the Bcl-2 and Bax interaction was fewer than half of that on the anti Bcl-2 and Bcl-2 interaction. The result is attributed to some reasons. One is probability of the biding. Since the probability of Bcl-2 binding with anti Bcl-2, and that of Bax binding with Bcl-2 were lower than 100 %, the

amount of analyte would decrease through the course of the interaction order. Secondly, the result might be depended on the diffusion factor of materials. Our results certify that QCM based sensor with the nano-honeycomb electrode having large surface area can detect frequency shifts corresponding to the PPI.

IV. CONCLUSION

We developed a novel and high-sensitivity QCM sensor with an AAO and honeycomb nanostructure. In addition, we successfully applied the electrode to assess PPIs between anti Bcl-2 and Bcl-2 and between Bcl-2 and Bax. These results indicate that the sensitivity of the QCM is improved using the sensor with the nano-honeycomb electrode because of its large surface area for binding with the analyte.

REFERENCES

[1] R. Kluger, A. Alagic, "Chemical cross-linking and protein-protein interactions – a review with illustrative protocols," *Bioorganic Chemistry*, vol. 32, pp. 451–472, 2004.

[2] K. L. Wegener, I. D. Campbell, "Transmenbrane and cytoplasmic domains in integrin activation and protein-protein interactions (Review), "*Molecular Membrane Biology*, vol. 25, pp. 376–387, 2008.

[3] X. Morelli, R. Bourgeas, P. Roche, "Chemical and structural lessons from recent successes in protein-protein interaction (2P2I)," *Curr. Opin. Chem. Biol.*, vol. 15, pp. 475−481, 2011.

[4] L. Laraia, G. McKenzie, D. R. Spring, A. R. Venkitaraman, D. J. Huggins, "Overcoming chemical, biological, and computational challenges in the development of inhibitors targeting protein-protein interations", *Chem. Biol.*, vol. 22, pp. 689−703, 2015.

[5] S. Hoelder, P. A. Clarke, P. Workman, "Discovery of small molecule cancer drugs: Successes, challenges and opportunities," *Molecular Oncology*, vol. 6, pp. 155–176, 2012.

[6] D. C. Fry, "Protein-protein interactions as targets for small molecule drug discovery,"*Biopolymers*, vol. 84, pp. 535–552, 2006.

[7] G. L. Verdine, G. J. Hilinski, "Stapled peptides for intracellular drug targets," *Methods Enzymol.*. vol. 503, pp. 3−33, 2012.

[8] K. F. Underwood, D. R. D'Souza, M. Mochin-Peters, A. D. Pierce, S. Kommineni, M. Choe, J. Bennett, A. Gnatt, B. Habtemariam, A. D. Mackerell, A. Passaniti, "Regulation of RUNX2 transcription factor-DNA interactions and cell proliferation by vitamin D3(cholecalciferol) prohormone activity,"*Journal of Bone and Mineral Research*, vol. 27, pp. 913–925, 2012.

[9] K. Sakamoto, S. Sogabe, Y. Kamaeda, N. Sakai, K. Asano, M. Yoshimatsu, K. Ida, Y. Imaeda, J. Sakamoto, "Discovery of high–affinity BCL6–binding peptide and its structure–activity relationship," *Biochem. Biophys. Research Commun.*, vol. 482, pp. 310–316, 2017.

[10] Y. Kamada, N. Sakai, S. Sogabe, K. Ida, H. Oki, K. Sakamoto, W. Lane, G. Snell, M. Iida, Y. Imaeda, J. Sakamoto, J. Matsui, "Discovery of a B–cell Lymphoma 6 Protein–Protein interaction Inhibitor by a Biophysics–Driven Fragment-Based Approach,"*J. Medical Chem.*, vol. 60, pp. 4358–4368, 2017.

[11] S. G. Patching, "Surface plasmon resonance spectroscopy for characterization of membrane protein-protein interactions and its potential for drug discovery," *Biochimica et Biophysica Acta-Biomembranes*, vol. 1838, pp. 43-55, 2014.

[12] I. Navratilova, A. L. Hopkins,"Emerging role of surface plasmon resonance in fragment-based drug discovery," *Future Medical Chem.*, vol. 3, pp. 1809–1820, 2011.

[13] J. A. Miles, D. J. Yeo, P. Rowell, S. Rodriguez-Marin, C. M. Park, S. L. Warriner, T. A. Edwards, A. J. Wilson, "Hydrocoarbon constrained peptides ― understanding preorganization and binding affinity," *Chemical Science*, vol. 7, pp. 3694-3702, 2016.

[14] T. Ito, N. Aoki, S. Kaneko, K. Suzuki, "Highly sensitive and rapid sequential cortisol detection using twin sensor QCM," *Anal. Methods*, vol. 6, pp. 7469–7474, 2014.

[15] N. Asai, H. Terasawa, T. Shimizu, S. Shingubara, T. Ito,"Sensitized mass change detection using Au nanoporous electrode for biosensing," *Jpn. J. Appl. Phys.*, vol. 56, 06GG04, 2017.

[16] N. Asai, H. Terasawa, T. Shimizu, S. Shingubara, T. Ito, "Highly sensitive quartz crystal microbalance based biosensor using Au dendrite structure," *Jpn. J. Appl. Phys.*, vol. 57, 02CD01, 2018.

[17] M. H. Kang, C. P. Reynolds, "Bcl-2 inhibitors: targeting mitochondrial pathways in cancer therapy," *Clin. Cancer Res.*, vol. 15, pp. 1126–1132, 2009.

[18] A. J. Souers, J. D. Leverson, E. R. Boghaert, S. L. Ackler, N. D. Carton, J. Chen, B. D. Dayton, H. Ding, S. H. Enschede, W. J. Fairbrother, D. C. S. Huang, S. G. Hymowitz, S. Jin, S. L. Khaw, P. J. Kovar, L. T. Lam, J. Lee, H. L. Maecker, K. C. Marsh, K. D. Mason, M. J. Mitten, P. M. Nimmer, A. Oleksijew, C. H. Park, C. –M. Park, D. C. Phillips, A. W. Roverts, D. Sampath, J. F. Seymour, M. L. Smith, G. M. Sullivan, S. K. Tahir, C. Tse, M. D. Wendt, Y. Xiao, J. C. Xue, H. Zhang, R. A. Humerickhouse, S. H. Rosenberg, S. W. Elmore, "ABT−199, a potent and selective BCL-2 inhibitor, archives antitumor activity while sparing platelets," *Nature Medicine*, vol. 19, pp. 202–208, 2013.

[19] J. Chen, H. Zhou, A. Aguilar, L. Liu, L. Bai, D. McEachern, C. –Y. Yang, J. L. Meagher, J. A. Stuckey, S. Wang, "Structure-based discovery of BM-957 as a potent small-molecule inhibitor of Bcl-2 and Bcl-xL capable of achieving complete tumor regression," *J. Med. Chem.,* vol. 55, pp. 8502 – 8514, 2012.

[20] P. H. Bernardo, K. –F. Wan, T. Sivaraman, J. Xu, F. K. Moore, A. W. Hung, H. Y. K. Mok, V. C. Yu, C. L. L. Chai, "Structure-activity relationship studies of phenanthridine-based Bcl-xL inhibitors," *J. Med. Chem.*, vol. 51, pp. 6699–6710, 2008.

[21] F. Edlich, S. Banerjee, M. Suzuki, M. M. Cleland, D. Arnoult, C. Wang, A. Neutzner, N. Tjandra, R. J. Youle, "Bcl-X$_L$ Retrotranslocates Bax from the Mitochondria into the Cytosol," *Cell*, vol. 145, pp. 104-116, 2011.

[22] F. A. C. G. Sousa, T. C. Paradella, Y. R. Carvalho, L. E. B. Rosa, "Comparative analysis of the expression of proliferating cell nuclear antigen, p53, bax, and bcl-2 in oral lichen planus and oral squamous cell carcinoma,"*Annals of Diagnostic Pathology*, vol. 13, pp. 308–312, 209.

[23] J.-F. Li, S.-J. Zheng, L.-L. Wang, S. Liu, F. Ren, Y. Chen, L. Bai, M. Liu, Z.-P. Duan*,* "Glucosylceramide synthase regulates the proliferation and apoptosis of liver cells in vitro by Bcl-2/Bax pathway," *Molecular Medicine Reports*, vol. 16, pp. 7355 – 7360, 2017.

[24] M. Kim, S. O. Jung, K. Park, E. J. Jeong, H.-A. Joung, T-H. Kim, D-W. Seol, B. H. Chung, "Detection of Bax protein conformational change using a surface plasmon resonance imaging-based antibody chip," *Biochemical and Biophysics Research Communications*, vol. 338, pp. 1834–1838, 2005.

[25] H. Ogi, K. Motoshisa, T. Matsumoto, K. Hatanaka, M. Hirao, "Isolated Electrodeless High-Frequency Quartz Crystal Microbalance for Immunosensors," *Anal. Chem.*, vol. 78, pp. 6903–6909, 2006.

[26] J. Liao, M. Lu, D. Tang, "Enhanced sensitivity of quartz crystal microbalance immunosensor via back-conjugation of biofunctionalized magnetic beads with an external magnetic field," *Biochemical Engineering Journal*, vol. 114, pp. 276–282, 2016.

[27] N. A. Masdor, Z. Altintas, I. E. Tothill, "Sensitive detection of *Campylobacter jejuni* using nanoparticles enhanced QCM sensor," *Biosens. Bioelectron.*, vol. 78, pp. 328–336, 2016.

[28] T. Ito, N. Yamanishi, T. Shimizu, S. Shingubara, "ZnO Nanostructure Based QCM sensor to Detect Ethanol at Room Temperature Facricated by All Wet Process," *Proceedings*, vol. 2017, pp. 397–400, 2017.

[29] K. N. Chappanda, O. Shekhan, O. Yassine, S. P. Patole, M. Eddaoudi, K. N. Salam, "The quest for highly sensitive QCM humidity sensors: The coating of CNT/MOF composite sensing films as case study," *Sens. Actuators B*, vol. 257, pp. 609–619, 2018.

[30] T. W. Chao, C. J. Liu, A. H. Hsieh, H. M. Chang, Y. S. Huang, D. S. Tsai, "Quartz crustal microbalance sensor based on nanostructured IrO2," *Sens. Actuators B*, vol. 122, pp. 95–100, 2007.

[31] A. Saedi, M. Ghorbani, "Electrodeposition of Ni-Fe-Co alloy nanowire in modified AAO template," *Mater. Chem. Phys.*, vol. 91, pp. 417–423, 2005.

[32] P. Hoyer, K. Nishio, H. Masuda, "Preparation of regularly structured porous metal menbranes with two different hole diameters at the tow sides," *Thin Solid Films*, vol. 286, pp. 88–91, 1996.

[33] S. Shingubara, S. Maruo, Y. Mayashita, M. Nakao, T. Shimizu, "Reduction of pitch of nanohole array by self-organizing anodic oxidation after nanoimprinting," *Microelectron. Eng.*, vol. 87, pp. 1451–1454, 2010.

[34] N. Asai, T. Shimizu, S. Shingubara, T. Ito, "Fabrication of highly sensitive QCM sensor using AAO nanoholes and its application in biosensing," *Sens. Actuators B*, vol. 276, pp. 534–539, 2018.

[35] J. Choi, R. B. Wehrspohn, U. Gösele, "Mechanism of guided self-organization producing quasi-monodomain porous alumina," *Electrochim. Acta*, vol. 50, pp. 2591–2595, 2005.

[36] Z. Balevicius, A. Paulauskas, I. Plikusiene, L. Mikoliunaite, M. Bechelany, A. Popov, A. Ramanavicius, A. Ramanavicience, "Towards the application of Al2/ZnO nanolaminates in immunosensors: total internal reflection spectroscopic ellipsometry based evaluation of BSA immonobilization," *J. Mater. Chem. C*, vol. 6, pp. 8778–8783, 2018.

Naoto Asai received B. E. degree from the Mechanical Engineering, Kansai University, Japan, in 2015 and M. E. degree in 2017, from Science and Engineering, Graduate school of Kansai University. He is now student in doctorial course in Science and Engineering, Kansai University. His research interest is biosensing devices with nanostructures.

Naohiro Mastumoto received B. E. degree from the Mechanical Engineering, Kansai University, Japan, in 2018. He is now student in Master course in Science and Engineering, Graduate school of Kansai University. His research interests are biosensing devices with nanostructures.

Nozomi Kazama received B. E. degree from the Chemistry, Materials and Bioengineering, Kansai University, Japan, in 2017. She is now student in Master course in Science and Engineering, Graduate school of Kansai University. Her research interest is developing a novel methodology to detect protein-protein interactions.

Yasuo Nagaoka received the B. Sci. degree from Meiji Pharmaceutical College, Japan, in 1989, the M. Sci. degree and Ph. D. degree from Graduate School of Pharmaceutical Sciences, Kyoto University, Japan, in 1991 and 1996, respectively. After the graduate, he had worked as a Research Associate in Faculty of Pharmaceutical Sciences in Kyoto University from 1992 to 2001 and as an Associate Professor in Faculty of Engineering of Kansai University from 2001 to 2010. He is currently a Professor in Department of Life Science and Biotechnology in Kansai University. He is interested in explorative study of useful bioactive compounds derived from natural resources.

Takaaki Sumiyoshi graduated from Faculty of Pharmaceutical Sciences, Kyoto University in 1999. He received the M. Sci. degree and Ph. D. degree from Graduate School of Pharmaceutical Sciences, Kyoto University, Japan, in 2001 and 2005, respectively. After the graduate, he had worked as a medicinal chemist in Dainippon Sumitomo Pharma from 2005 to 2014. He is now an Associate Professor in Department of Life Science and Biotechnology in Kansai University from 2014. He is interested in medicinal chemistry.

Tomohiro Shimizu received M.S. degree (Physics) in Nihon University and Ph.D. (Material Science) from Hiroshima University, Japan, in 2003 and 2006, respectively. After the graduate, he was post-doctoral researcher in Max-Planck Institute from 2006 to 2008. He worked as assistant professor from 2010 to 2013 in Kansai University, is now associate professor in Kansai University. His research interests are functional nanostructures for green energy such as solar cell and electronic devices.

Shoso Shingubara graduated from Bachelor course of the department of pure and applied science, the University of Tokyo in 1980. He received Ph.D. from the department of applied physics, Tokyo Institute of Technology in 1985. After graduation, he joined Toshiba ULSI research center as a researcher, and engaged in R &D of LSI multilevel interconnection technologies. Then he moved to Hiroshima University, department of electrical engineering as an associate professor in 1990. He moved to Kansai University, department of mechanical engineering as a full professor in 2005. His research interests are focused on nanostructure fabrication using wet-chemical self-organizing methods, and their application to sensors, 3D interconnections, as well as functional devices such as nonvolatile memories and neuromorphic devices.
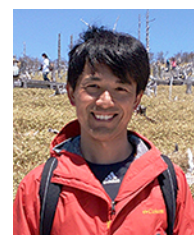
Takeshi Ito received B. Sci. from Earth and Space Science in Osaka University, Japan, in 1995. He received M. Sci. from Earth and Planetary Physics from the University of Tokyo, in 1997. After the graduate, he had worked as a researcher in Kanagawa Industrial Technology Institute from 1997 to 2014. Among then, he received Dr. Eng. from Graduate school of Science and Technology, Keio University, Japan, in 2007. He worked as associate professor in Kansai University from 2015 to 2017, is now full professor in Kansai University from 2018. His research interests are biosensing devices using nanostructures and interfaces between solid and biomaterials.